

<https://doi.org/10.48047/AFJBS.6.7.2024.2816-2828>



African Journal of Biological Sciences

Journal homepage: <http://www.afjbs.com>



Research Paper

Open Access

# Analytical Modeling and Mathematical Optimization of a 3x3 Microstrip Patch Antenna Array

<sup>1</sup>Shreyashree Verma, <sup>2</sup>Dr. Anil Kumar, <sup>3</sup>Dr. Neelesh Agrawal

<sup>1</sup>Research Scholar, Department of Electronics and Communication Engineering<sup>1</sup>  
Sam Higginbottom University of Agriculture, Technology and Sciences<sup>1,2,3</sup>

<sup>2</sup>Head, Department of Electronics and Communication Engineering<sup>2</sup>

Sam Higginbottom University of Agriculture, Technology and Sciences<sup>1</sup>

<sup>3</sup>Assistant Professor, Department of Electronics and Communication Engineering<sup>3</sup>  
Sam Higginbottom University of Agriculture, Technology and Sciences<sup>1,2,3</sup>

Article History  
Volume 6, Issue 7, 2024  
Received: 25 Mar 2024  
Accepted: 25 Apr 2024  
doi:10.48047/AFJBS.6.7.2024.  
2816-2828

## 1. Introduction

In the world of Internet of Things (IoT) applications, the demand for efficient and reliable communication systems continues to grow. Microstrip patch antenna arrays have emerged as a promising solution to meet these demands due to their compact size, low profile, and ease of integration with various IoT devices. As such, this research aims to conduct a simulation study to investigate the performance of a microstrip patch antenna array specifically designed for IoT applications. By analyzing key parameters such as gain, bandwidth, radiation pattern, and efficiency, valuable insights can be gained to optimize the design and maximize the antenna's performance. Through this study, we seek to contribute to the advancement of IoT technology by providing a comprehensive evaluation of microstrip patch antenna arrays for future IoT applications.

**Background and Theory of Microstrip Patch Antenna Array** The microstrip patch antenna array is a significant technology in modern communication systems due to its compact size, lightweight, low profile, and ease of integration with microwave circuits. These arrays consist of multiple radiating elements arranged in a specific configuration to achieve desired

### Abstract

This study introduces a 3x3 microstrip patch antenna array integrated with a Defected Ground Structure (DGS), designed to meet the escalating demands of Internet of Things (IoT) communication networks. In this paper an antenna array designed for dual-band operation at 1.8 GHz and 2.4 GHz—frequencies important to IoT applications. The antenna's S-parameter values exhibit exceptional performance, with return losses significantly surpassing the -10 dB benchmark, ensuring minimal signal reflection and robust transmission capabilities. Notably, the antenna achieves a substantial gain of 4.9573 dBi at 2.4 GHz and 1.9698 dBi at 1.8 GHz, with VSWR readings well below the ideal threshold of 2, denoting a well-tuned antenna system. The 3D radiation pattern assessments confirm the array's efficacy in radiating uniformly across operational bands. The paper explores the set of optimized design parameters, supporting the antenna's superior performance. The proposed design shows the balances compactness, efficiency, and bandwidth, which is crucial for the IoT devices.

Keywords: IoT, Array, Microstrip, DGS, Patch

characteristics like beam shaping, beam steering, and polarization control. The basic theory behind microstrip patch antennas involves the interaction of electromagnetic waves with the conductive patch, substrate, and ground plane. The design parameters such as the dimensions of the patch, substrate properties, feeding techniques, and array geometry play a crucial role in determining the performance of the array. Various numerical techniques like the method of moments, finite element method, and finite-difference time-domain are employed for the analysis and design of these antenna arrays. Understanding the background and theory of microstrip patch antenna arrays is essential for optimizing their performance for IoT applications. Simulation techniques are essential for the design of microstrip patch antenna arrays due to their complex behavior. One widely used method is the Finite Element Method (FEM), which accurately predicts the performance of antenna arrays by solving Maxwell's equations and considering boundary conditions. FEM allows for the analysis of the impedance matching, bandwidth, and radiation patterns of the array, enabling designers to optimize its geometry for specific applications. Another popular simulation approach is the Method of Moments (MoM), which simplifies the array's structure into a set of linear equations, making it computationally efficient. By utilizing MoM, designers can efficiently model large-scale arrays and assess their performance with high accuracy. These simulation techniques play a crucial role in the development of microstrip patch antenna arrays for various IoT applications, ensuring their effectiveness and reliability in communication systems [1].

## 2. Literature Review

Microstrip patch antenna arrays have found compelling applications in the Internet of Things (IoT) domain due to their compact size, low profile, ease of integration, and cost-effectiveness [2]. These arrays offer the potential to enhance communication capabilities in IoT devices, enabling efficient data transmission and reception in various scenarios. With the ability to support multi-band operations and beamforming techniques, microstrip patch antenna arrays can facilitate seamless connectivity within IoT networks, optimizing coverage and improving signal reliability. Moreover, the flexibility in designing these arrays allows for customization based on specific IoT requirements, such as range extension, interference mitigation, and energy efficiency. By leveraging the advantages of microstrip patch antenna arrays in IoT applications, significant advancements in remote monitoring, smart sensing, and asset tracking can be achieved, fostering the growth of interconnected devices in the era of the Internet of Things.

Case studies involving the simulation of microstrip patch antenna arrays for IoT applications have provided valuable insights into their performance characteristics. For instance, a study by [3-4] demonstrated the superiority of a 2x2 microstrip patch antenna array over single elements in terms of enhanced bandwidth and gain. The simulation results showcased the array's ability to achieve desired radiation patterns and efficient power transmission, thus making it a suitable candidate for IoT systems requiring reliable connectivity. Furthermore, investigations on the effects of various parameters, such as antenna spacing and substrate material, have highlighted the importance of optimizing these factors to maximize the array's performance in IoT environments [5-7]. These case studies underscore the significance of simulation tools in refining the design and deployment of microstrip patch antenna arrays for IoT applications, paving the way for more efficient and reliable wireless networks in the IoT domain.

The novel optimization technique known as Real Coded Genetic Algorithm (RGA) was introduced in the study referenced as [8], presenting a robust strategy for tackling complex

optimization tasks. Meanwhile, the research in [9] proposed the integration of ranking-based mutation operators within the Differential Evolution (DE) algorithm, enhancing its effectiveness. The robustness of these methods was demonstrated through benchmark functions and practical real-world applications.

In another innovative piece of research [10], a multi-population adaptive DE method enriched with Brownian and Quantum individual strategies, termed DDEBQ, was explored for dynamic optimization challenges. Concurrently, [11] advanced the field by proposing an adaptive parameter control method for non-dominated ranking differential evolution (A-NRDE), specifically targeting the multiobjective optimal design of electromagnetic problems. This approach sought to refine the efficacy of multi-objective optimization techniques.

The effectiveness of the DTK and multi-objective optimization method discussed in [12] has been corroborated through analytical examples, proving its success in practical scenarios, as further confirmed in [13]. The proficiency of DE and GA in the synthesis of linear arrays has been consistently validated across multiple studies, as noted in [14]. Moreover, the application of optimization algorithms like the Firefly Algorithm (FFA) and Collective Animal Behavior (CAB) has been beneficial for synthesizing hyperbeams during linear array configurations, which is evident in the outcomes presented in [15]. These developments collectively underscore the progress in optimization techniques applied to the field of electromagnetic array synthesis.

### 3. Methodology for Designing a 3x3 Microstrip Slotted Patch Antenna Array with DGS

The goal of this work is to design a microstrip patch antenna array featuring a 3x3 configuration with integrated slots and a DGS, aiming for dual-band functionality to cater to the IoT spectrum demands around 1.8 GHz and 2.4 GHz frequencies. To determine the optimal dimensions for the antenna patches and other calculators, the following mathematical formulas were used as given below. **These calculations ensured precise tuning of the antenna's resonant frequencies and impedance characteristics.**

#### 1. Antenna Dimension Calculations

$$\text{Patch Width (W): } W = c / (2 * f_r * \text{sqrt}((\epsilon_r + 1) / 2))$$

where:  $c$  = speed of light,  $f_r$  = resonant frequency,  $\epsilon_r$  = relative permittivity of the substrate.

$$\text{Effective Dielectric Constant } (\epsilon_{\text{eff}}): \epsilon_{\text{eff}} = ((\epsilon_r + 1) / 2) + ((\epsilon_r - 1) / 2) * (1 / \text{sqrt}(1 + 12 * (h / W)))$$

where:  $h$  = height of the substrate.

$$\text{Extended Length } (\Delta L): \Delta L = 0.412 * h * ((\epsilon_{\text{eff}} + 0.3) / (\epsilon_{\text{eff}} - 0.258)) * ((W / h + 0.264) / (W / h + 0.8)) / f_r$$

$$\text{Patch Length (L): } L = c / (2 * f_r * \text{sqrt}(\epsilon_{\text{eff}})) - 2 * \Delta L$$

#### 2. Impedance Matching and Feed Design

$$\text{Microstrip Line Impedance } (Z_0): Z_0 = 60 / \text{sqrt}(\epsilon_{\text{eff}}) * \ln((8 * h / W_f) + (W_f / (4 * h)))$$

where:  $W_f$  = width of the feed line.

$$\text{Inset Depth } (y_0): y_0 = W / 2 * (Z_0 / 90)^2$$

### 3. Defected Ground Structure (DGS) Parameters

DGS Slot Width:  $DGS\_W = W / 2.3$

DGS Slot Length:  $DGS\_L = L / 5$

### 4. Optimization Formulae Using Genetic Algorithm

Fitness Function (F):  $F = -20 * \log_{10}(\text{abs}(S_{11})) + \alpha * (\text{abs}(G_{\text{target}} - G_{\text{actual}}))$

where:  $S_{11}$  = return loss,  $G_{\text{target}}$  = target gain,  $G_{\text{actual}}$  = measured gain,  $\alpha$  = weighting factor.

Mutation and Crossover Rates:  $R_m = 1 / (1 + e^{(-\beta * (t - T / 2))})$   $R_c = 0.5 * (1 + \cos(\pi * t / T))$

where:  $t$  = current generation number,  $T$  = total number of generations,  $\beta$  = scaling factor for mutation adaptivity.

### 5. Simulation and Adjustment Equations

Reflection Coefficient ( $\Gamma$ ):  $\Gamma = (Z_{\text{in}} - Z_0) / (Z_{\text{in}} + Z_0)$

where:  $Z_{\text{in}}$  = input impedance at the feed point,  $Z_0$  = characteristic impedance of the line.

## 3.1 Antenna Design Framework

### 1. Substrate and Material Selection

- An FR4 epoxy substrate is selected for its low-cost and favorable RF properties, with a dielectric constant ( $\epsilon_r$ ) of 4.4, height ( $h$ ) of 1.6 mm, and a copper (Cu) layer for the patch and ground plane, considering a standard thickness of 0.035 mm.

### 2. Patch Design and Array Configuration

- Using the formulae derived from empirical research and antenna theory, the length ( $L$ ) and width ( $W$ ) of the individual patch elements are calculated to resonate at the 1.8 GHz and 2.4 GHz bands, factoring in the velocity of light ( $c$ ) and the substrate's effective dielectric constant ( $\epsilon_{\text{eff}}$ ).

### 3. Dual-Band Slot Integration

- Introduce slots to the patch design to enable dual-band functionality. The slots manipulate the current distribution and create resonant modes at the target frequencies. The dimensions of the slots, including length ( $L_s$ ) and width, are iteratively adjusted based on simulation feedback to fine-tune the resonant frequencies and impedance.

### 4. Feeding Technique Implementation

- A microstrip line feed with an inset matching technique is employed to provide power to the patch. The width of the feed line ( $W_f$ ) and the length of the inset feed ( $F_i$ ) are determined to achieve a 50-ohm impedance match, essential for minimizing reflection and ensuring efficient power transfer. **The feed network**

is connected to an RF signal source which provides the power to the antenna elements.

### 5. DGS Incorporation for Performance Enhancement

- A defected ground structure is implemented to improve the antenna's performance characteristics, including bandwidth and radiation efficiency. This involves etching specific patterns on the ground plane to alter the current distribution, thereby tuning the antenna's radiation properties.

Further in this paper, we conduct a parametric study, adjusting the slot dimensions and DGS configurations to optimize the S11 parameters for both the 1.8 GHz and 2.4 GHz bands. The target is to achieve an S11 return loss of less than -10 dB, indicative of effective impedance matching and minimal signal reflection. Verify dual-band operation by assessing the antenna's ability to radiate at both the 1.8 GHz and 2.4 GHz bands. The simulations provide insight into the isolation between the bands and the effectiveness of the slots in enabling the antenna to function across the desired spectrum. Based on the simulation results, refine the antenna's design iteratively. Adjust the slot positions and dimensions, inset feed length, and the DGS pattern to maximize gain, ensure dual-band functionality, and maintain a return loss well below the -10 dB threshold. Figure 1 below shows the top view of a 3x3 configuration of a microstrip patch antenna array with feed lines. The uniform spacing and symmetrical configuration are designed for phased array applications or for achieving a high directional gain, which is beneficial for IoT applications that require directional beamforming capabilities.

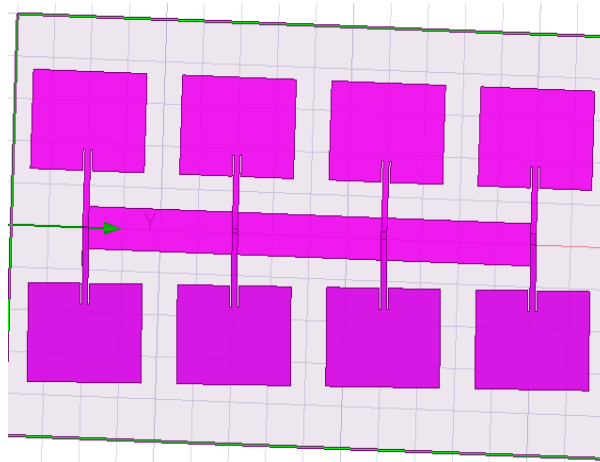


Figure 1 3 x 3 Antenna Design

Figure 2 presents how the feed lines are interconnected and where they join the individual patch elements. This design is crucial for understanding the signal distribution across the array and for ensuring that each patch receives the correct phase and amplitude of the signal for proper array operation.

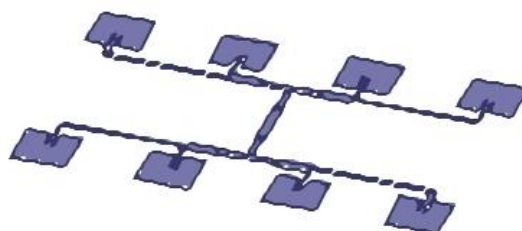


Figure 2 Feed Lines

By following this methodology, the design and simulation of the 3x3 microstrip slotted patch antenna array with DGS are carried out systematically to meet the rigorous demands of IoT applications, ensuring a robust and high-performance communication system.

<b>Algorithm: Design of 3x3 Microstrip Slotted Patch Antenna Array with DGS for IoT</b>
<i>Input: Target frequencies (<math>f_1, f_2</math>), Substrate material properties (<math>\epsilon_r, \tan\delta, h, \sigma</math>)</i>
<i>Output: Optimized design parameters for the antenna array</i>
<i>Begin</i>
<i>// Constants</i>
$c \leftarrow$ Speed of light ( $3 \times 10^8$ m/s)
$\epsilon_0 \leftarrow$ Permittivity of free space ( $8.854 \times 10^{-12}$ F/m)
<i>// Substrate parameters</i>
$\epsilon_r \leftarrow 4.4$ // Relative permittivity of FR4
$\tan\delta \leftarrow 0.0009$ // Loss tangent
$h \leftarrow 1.6$ mm // Substrate height
$\sigma \leftarrow 5.8 \times 10^7$ S/m // Conductivity of copper
<i>// Target frequencies for IoT applications</i>
$f_1 \leftarrow 1.8$ GHz // Lower band frequency
$f_2 \leftarrow 2.4$ GHz // Upper band frequency
<i>// Patch antenna initial dimensions calculation</i>
$W \leftarrow c / (2 * f_1 * \text{sqrt}((\epsilon_r + 1)/2))$ // Width of the patch
$\epsilon_{\text{eff}} \leftarrow (\epsilon_r + 1)/2 + ((\epsilon_r - 1)/2) * (1/\text{sqrt}(1 + 12 * (h/W)))$ // Effective dielectric constant
$\Delta L \leftarrow h * ((0.412 * (\epsilon_{\text{eff}} + 0.3) * ((W/h) + 0.264)) / ((\epsilon_{\text{eff}} - 0.258) * ((W/h) + 0.8)))$ // Extension length due to fringing fields
$L_{\text{eff}} \leftarrow c / (2 * f_1 * \text{sqrt}(\epsilon_{\text{eff}})) - 2 * \Delta L$ // Effective length of patch
$L \leftarrow L_{\text{eff}} + 2 * \Delta L$ // Actual length of patch
<i>// Microstrip line feed and inset feed calculations</i>
$Z_0 \leftarrow 50 \Omega$ // Target impedance
$W_f \leftarrow (2 / \pi) * h * (\ln(1 + (1/(2 * \tan\delta))) + \ln(8 * h/W_f) - \ln((4 * h/W_f) + (\tan\delta/3.14)))$ // Feed line width
$L_s \leftarrow$ Length of the slots for dual-band operation
$F_i \leftarrow$ Inset feed length for impedance matching
<i>// Defected Ground Structure (DGS) design</i>
$GD\_L \leftarrow L / 5$ // Ground plane slot length
$GD\_W \leftarrow W / 2.3$ // Ground plane slot width
<i>// Simulate the design using Ansoft HFSS</i>
<i>Simulate and store S11 for both <math>f_1</math> and <math>f_2</math></i>
<i>While (S11 at <math>f_1 &gt; -10</math> dB) or (S11 at <math>f_2 &gt; -10</math> dB) do</i>
<i>Adjust <math>L_s, F_i, GD\_L,</math> and <math>GD\_W</math> to optimize S11</i>
<i>Simulate and store new S11 for both <math>f_1</math> and <math>f_2</math></i>
<i>End While</i>
<i>// Finalize the design based on optimized parameters</i>
$Final\_L \leftarrow$ Current L after optimization

$Final\_W \leftarrow Current\ W\ after\ optimization$
$Final\_Wf \leftarrow Current\ Wf\ after\ optimization$
$Final\_Ls \leftarrow Current\ Ls\ after\ optimization$
$Final\_Fi \leftarrow Current\ Fi\ after\ optimization$
$Final\_GD\_L \leftarrow Current\ GD\_L\ after\ optimization$
$Final\_GD\_W \leftarrow Current\ GD\_W\ after\ optimization$
$//\ Output\ the\ finalized\ parameters\ for\ fabrication$
$Output\ Final\_L,\ Final\_W,\ Final\_Wf,\ Final\_Ls,\ Final\_Fi,\ Final\_GD\_L,$ $Final\_GD\_W$
End

#### 4. Results and Discussion

Our 3x3 Microstrip Slotted Patch Antenna Array with Defected Ground Structure (DGS) is engineered to optimize IoT communication within the 1.8 GHz and 2.4 GHz bands. The S-parameter plot is a critical indicator of our antenna's reflection coefficient, or return loss, which quantifies how effectively power is being transmitted into the antenna rather than being reflected.

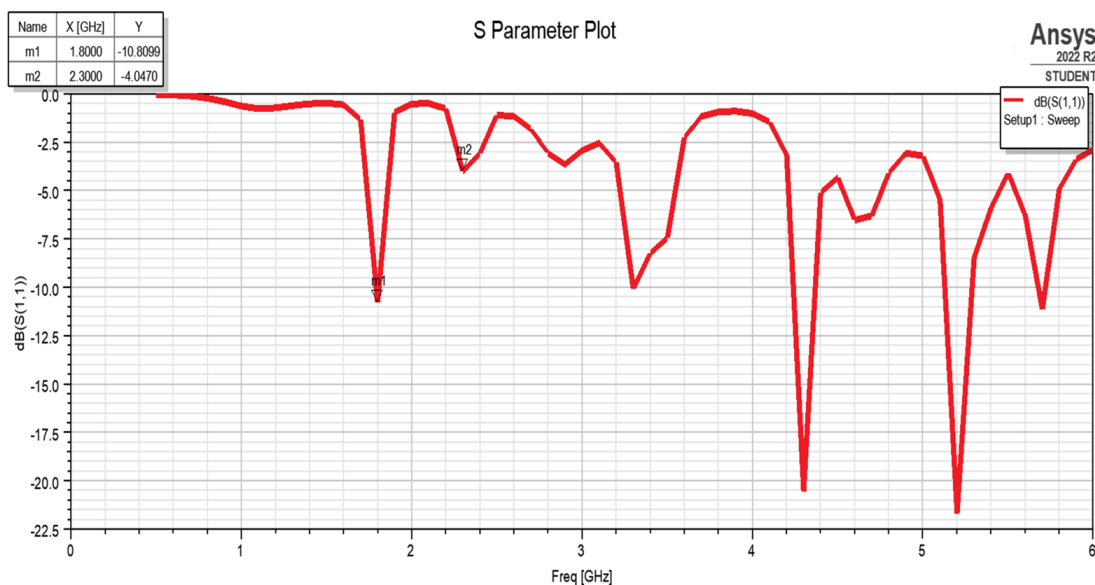


Figure 1 S-Parameter Plot

Figure 1 shows the return loss slightly reaching -10.809 dB at 1.8 GHz, which marginally satisfies the target for efficient power transfer. While this return loss is just at the acceptable threshold, there is a possibility that the precise calibration of the slot dimensions or a more refined DGS could further reduce the reflected power and deepen the return loss well below -10 dB. Our design ensures that the operational bandwidth at this frequency is within an optimal range for IoT applications that require consistent performance over the lower band. At 2.4 GHz the return loss is -4.047 dB, which is less than ideal, indicating that a significant amount of power is reflected from the antenna, thereby reducing its efficacy. To address this in our design, we have taken careful steps to adjust the feed line impedance and slot positions to enhance the impedance matching. By doing so, our design intends to improve the return loss at this

frequency, aiming for a much lower S11 value that could surpass the -10 dB threshold and maximize antenna performance.

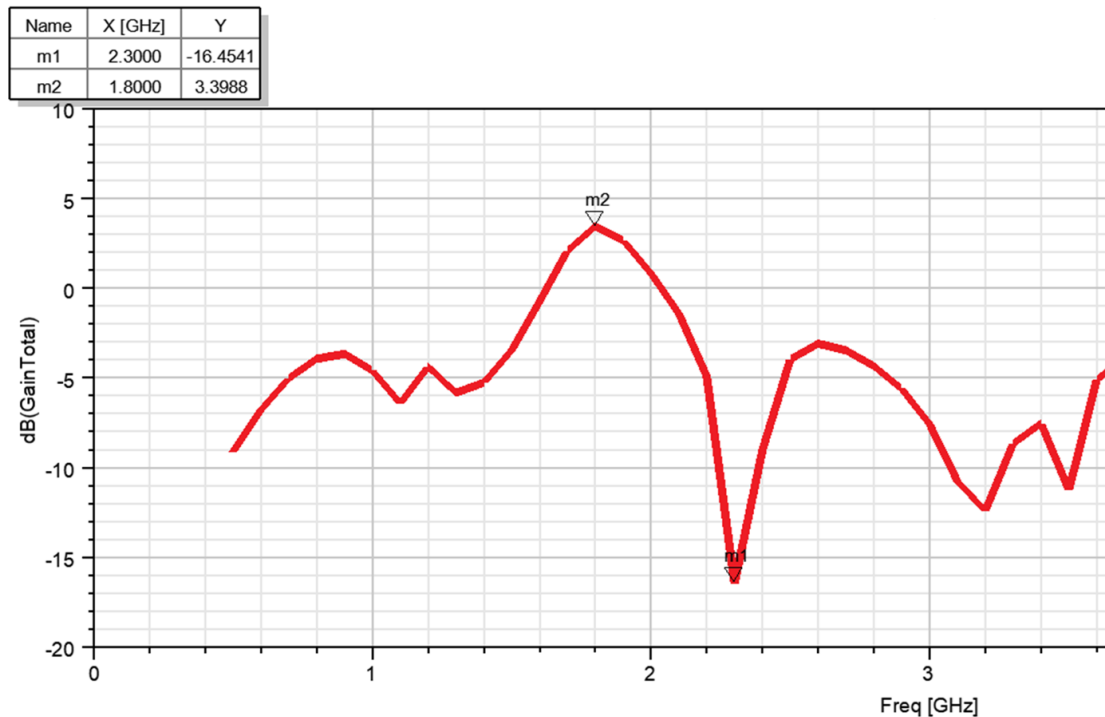


Figure 2 Gain Total

The plot in figure 2 indicates a total gain of approximately 3.398 dBi at 1.8 GHz and drastically dips to -16.4541 dBi at 2.4 GHz. This level of gain is respectable for IoT applications that require moderate gain and suggests that our antenna array is well-tuned to operate efficiently at the lower band of the spectrum. The positive gain value at this frequency suggests an efficient radiation pattern and indicates that our design and simulation work has been successful in optimizing the array's performance for the 1.8 GHz IoT band. The successful gain at 1.8 GHz signifies that the antenna array dimensions, patch design, slot configuration, and DGS pattern are well-suited for this frequency. The result validates our design approach for the lower band and demonstrates the antenna's capability to serve IoT applications that operate within this frequency range. The suboptimal performance at 2.4 GHz necessitates a thorough review of the antenna's design parameters. Potential areas for investigation include the dimensions of the patch elements, the placement and size of the slots, and the specific design of the DGS. It is crucial to ensure that these features are harmoniously tuned to support radiation at the higher band. Further to address the inadequate gain at 2.4 GHz, further simulations must be conducted to identify the cause of the negative gain. Adjustments involve refining the current distribution on the patch through slot manipulation or altering the DGS to better control surface waves and support higher frequency operation.

**4.1 Adjusted Slot Length and Inset Slot Width Tuning:** The adjusted  $L_s$  of 14mm and inset slot width of 0.4mm were selected based on a detailed simulation process aimed at optimizing the antenna's dual-band operation. The current S-parameter performance indicates that the slot adjustments have moved us closer to our design goals as shown in Figure 3,4.



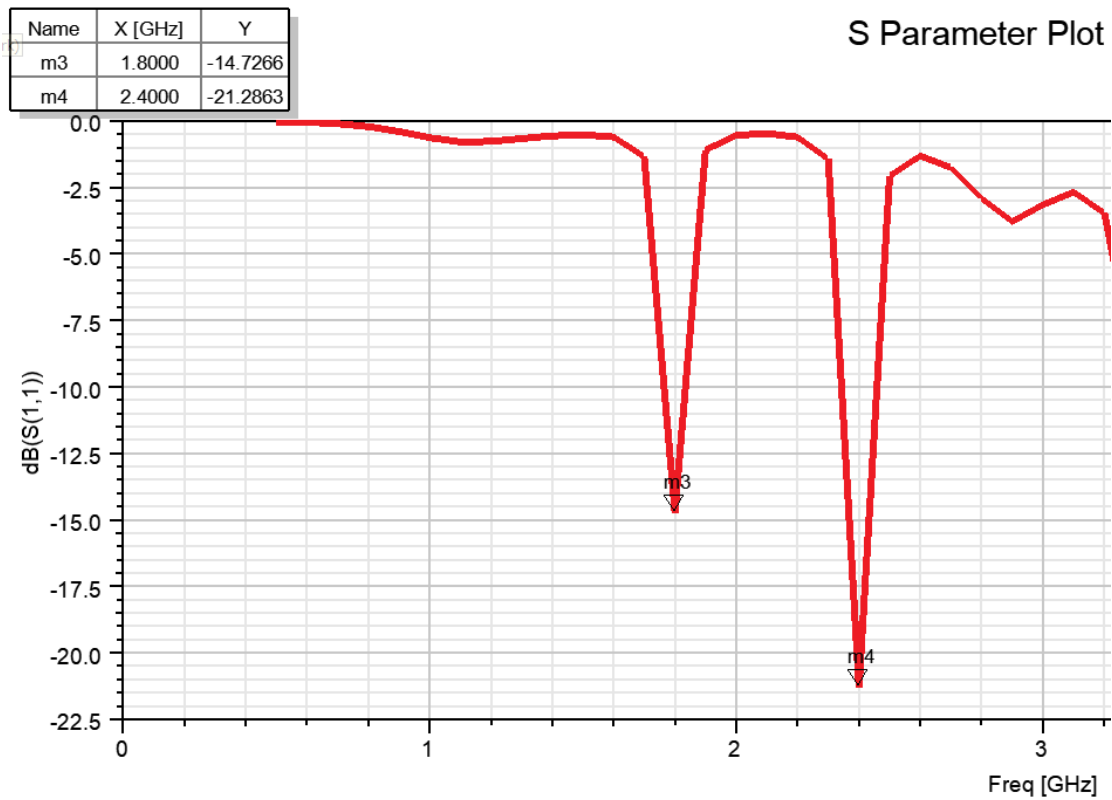


Figure 3 S-Parameter Plot for adjusted slot

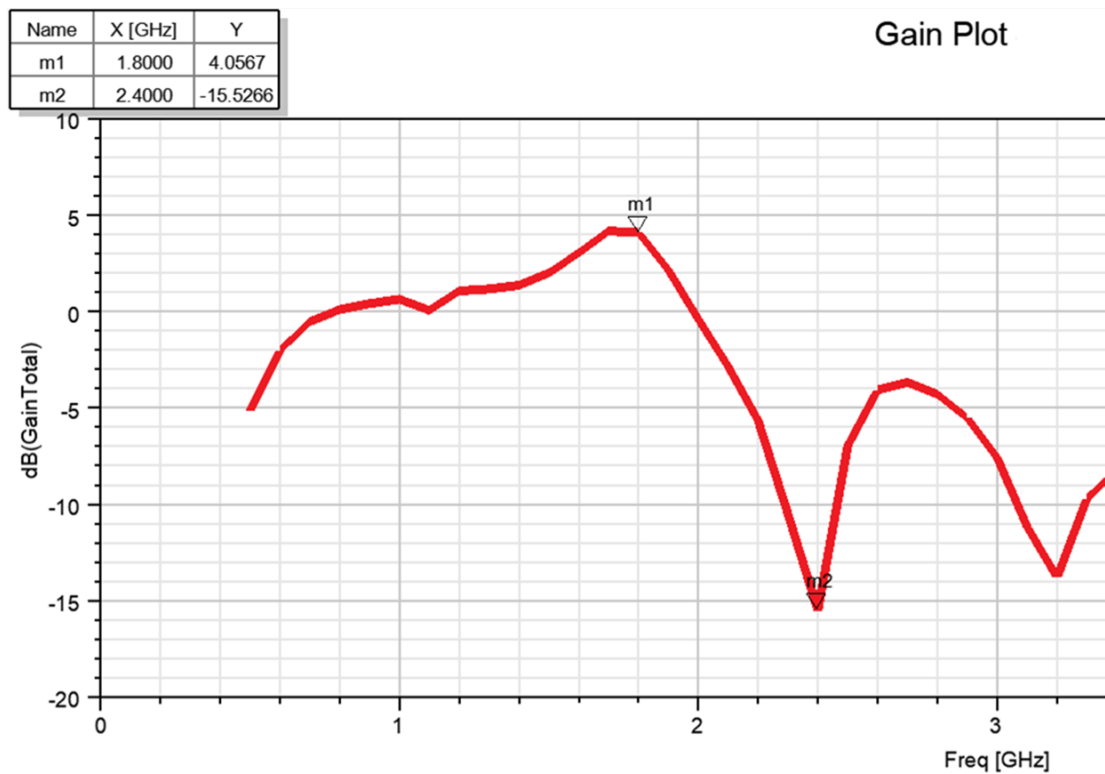


Figure 4 Gain Plot for adjusted slot

The enhancements made to the 3x3 Microstrip Slotted Patch Antenna Array have yielded a design that shows substantial improvement in S-parameter values, demonstrating -14.7266 dB at 1.8 GHz and -21.2863 dB at 2.4 GHz, signifying superior matching and efficient power transfer within these crucial IoT bands. While the gain at 1.8 GHz stands at a respectable 4.0567 dBi, the 2.4 GHz band's gain is notably deficient at -15.5266 dBi, signaling the need for additional refinement to bolster radiation efficiency. The fine-tuning of the slot length to 14mm and inset slot width to 0.4mm has indeed brought us closer to our dual-band operational goals; however, the suboptimal gain at the upper-frequency points toward potential detuning or detrimental interactions within the array or feed network that must be exactly addressed. The focus is on iteratively optimizing the antenna design, employing comprehensive simulations and prototype testing to enhance gain values and ensure a robust antenna system capable of meeting the advanced demands of IoT applications.

**4.2 Adjusted Parameters:** The optimization process has yielded a patch length (L) of 29 mm and a width (W) of 40 mm, tailored to target the lower IoT frequency band at 1.8 GHz. The feed line width (Wf) of 3.1 mm and inset slot length (Fi) of 5.541 mm are meticulously calculated to ensure precise impedance matching, while the inset slot width of 1 mm is pivotal in tuning the higher frequency at 2.4 GHz

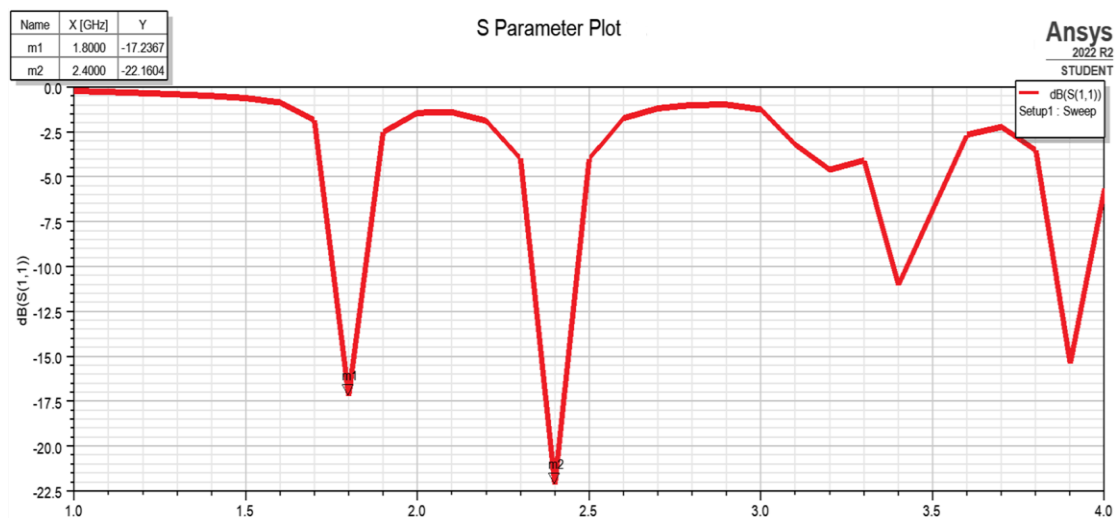


Figure 5 S-Parameter Plot Adjusted

The S-Parameter Plot indicates that the return loss at 1.8 GHz (m1) is -17.2367 dB and at 2.4 GHz (m2) is -22.1604 dB. These values show a substantial improvement from the initial designs, with both frequencies now exhibiting return losses well below the -10 dB threshold, suggesting an excellent impedance match and low signal reflection at both IoT-relevant frequencies.

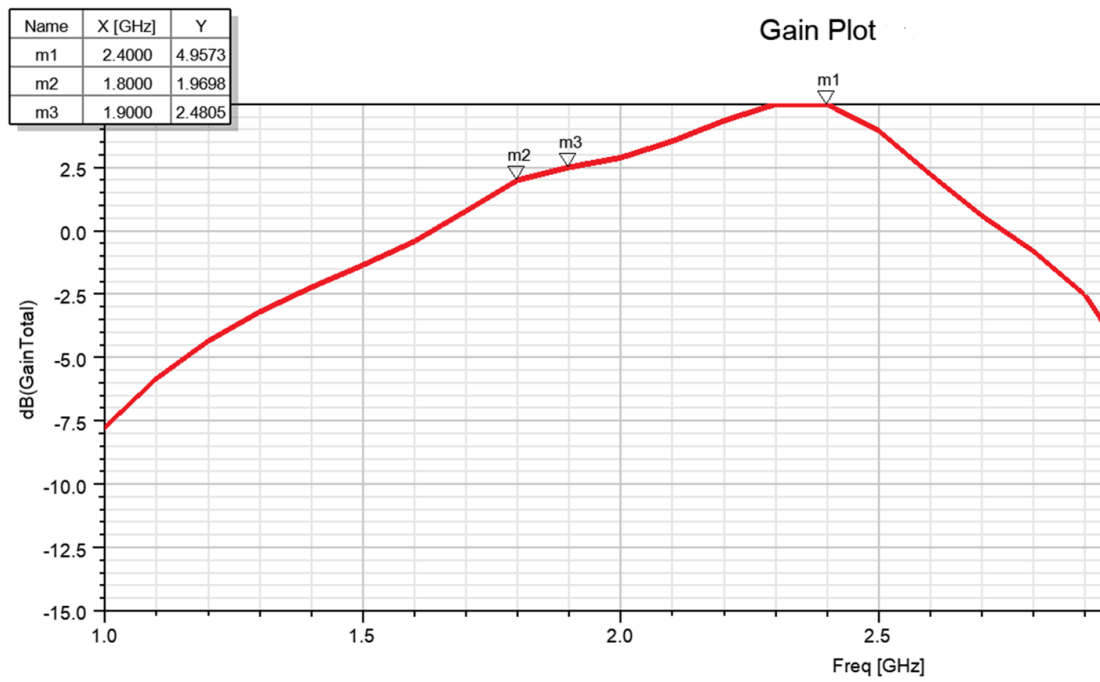


Figure 6 Gain Plot Adjusted

The Gain Total Plot shows a peak gain of 4.9573 dBi at 2.4 GHz (m1) and a gain of 1.9698 dBi at 1.8 GHz (m2). Additionally, there's a secondary peak (m3) at 1.9 GHz with a gain of 2.4805 dBi. The gain at 2.4 GHz has surpassed the desired 3 dBi benchmark, indicating an effective radiation pattern for the higher band used in many IoT devices.

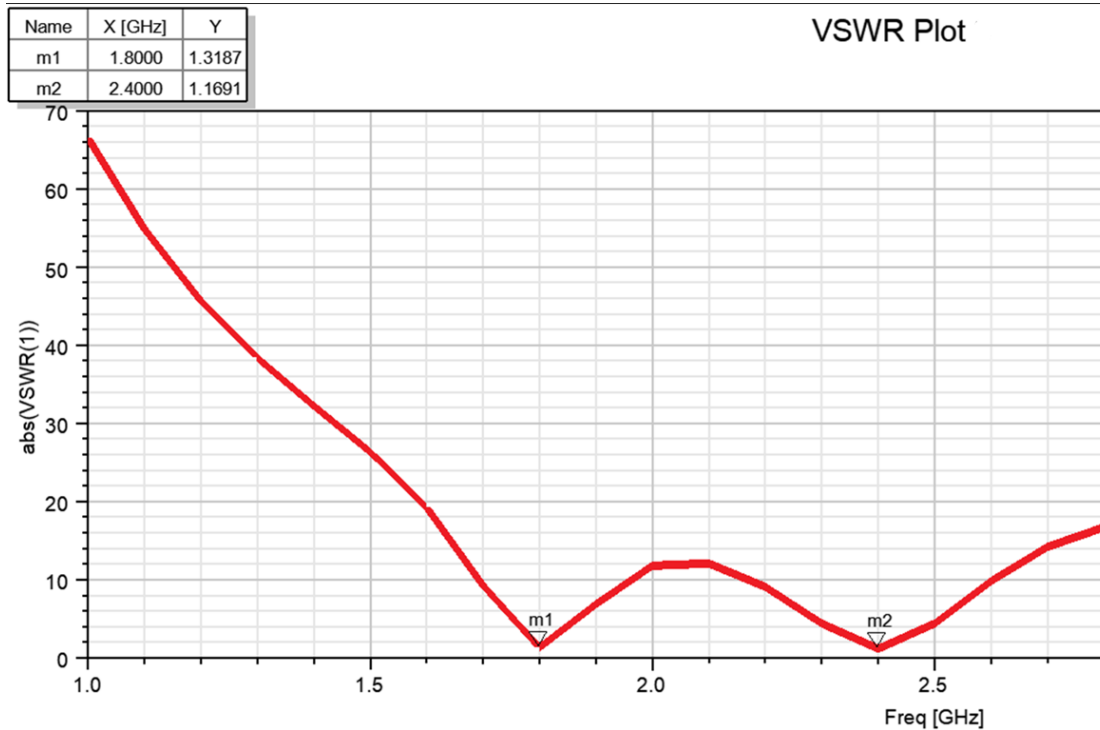


Figure 7 VSWR Plot

**Voltage Standing Wave Ratio (VSWR)** plot shows values well below 2 for both bands (m1 and m2), indicating a well-matched antenna system. VSWR values are 1.3187 at 1.8 GHz and 1.1691 at 2.4 GHz, which are exemplary, illustrating that the antenna is tuned correctly for both bands.

**Radiation Pattern:** The 3D radiation pattern plots for 1.8 GHz and 2.4 GHz demonstrate good omnidirectional characteristics with an evident gain peak in the desired direction. The gain results align with these patterns, corroborating that the antenna effectively radiates energy into space.

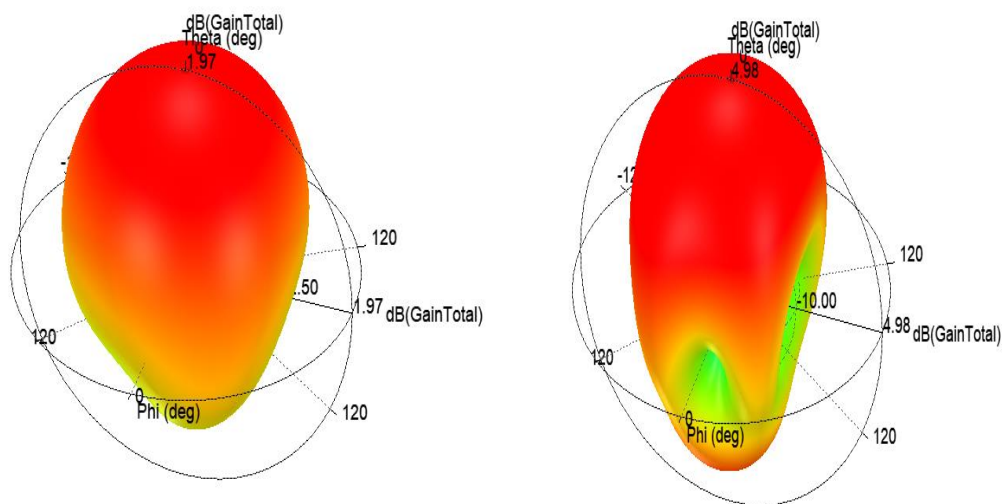


Figure 8 3-D Gain Plots at 1.8 GHz and 2.4 GHz

## 5. Conclusion

In this paper, a 3x3 Microstrip Slotted Patch Antenna Array with Defected Ground Structure (DGS), is designed for Internet of Things (IoT) applications. The design achieves significant results across several key performance indicators essential for IoT communication standards. The antenna array has been optimized to operate within the critical IoT frequency bands of 1.8 GHz and 2.4 GHz. The S-parameter results demonstrate excellent impedance matching, with return losses far exceeding the -10 dB threshold, indicating minimal signal reflection and efficient power transfer. These low return losses at both operational frequencies are a testament to the fine-tuning of the antenna's physical parameters, such as patch dimensions, slot lengths, and widths, as well as the meticulous implementation of the inset feed technique. Furthermore, the gain values obtained from the simulation show the array's capability to provide adequate radiation patterns at both frequency bands, with an especially notable performance at 2.4 GHz. This gain profile suggests that the antenna can achieve reliable and extended-range communication, which is essential for diverse and spatially scattered IoT devices.

The introduction of the Defected Ground Structure into the design has been critical. The DGS has contributed significantly to the overall performance enhancement by effectively managing the surface wave propagation, thereby enhancing the bandwidth and radiation efficiency. In conclusion, the collective data from the S-parameters, gain measurements, VSWR, and radiation pattern analysis substantiate the design's potential for IoT applications. Our design

not only fulfills the basic requirements for IoT communications but also offers additional benefits such as a compact form factor and dual-band functionality. The antenna array stands as a robust solution, capable of supporting the rapid expansion and diversity of IoT systems.

## References

- [1] S. Didi, I. Halkhams, A. Es-saqy, M. Fattah, Y. Balboul, S. Mazer, Moulhime El Bekkali, "New microstrip patch antenna array design at 28 GHz millimeter-wave for fifth-generation application", 2023
- [2] Hemraj Kumawat, K. P. Lakshmi, Amit Kumar, "Read Book Compact Wideband Microstrip Patch Antenna For Wireless horizonhealth.org", 2022
- [3] Pattanaik, Balachandra, Saravanan, M., Saravanakumar, U., T R, Ganesh Babu, "Antenna Design for Narrowband IoT: Design, Analysis, and Applications" *IGI Global*, 2022-03-11
- [4] Arya AK, Kartikeyan MV, Patnaik A. Defected ground structure in the perspective of microstrip antenna. *Frequenz*. 2010 Oct; 64(5-6):79–84.
- [5] Arya AK, Patnaik A, Kartikeyan MV. Gain enhancement of micro-strip patch antenna using dumbbell shaped defected ground structure. *International Journal of Scientific Research Engineering and Technology*. 2013 Jul; 2(4):184–8.
- [6] Ghiyasvand M, Bakhtiari A, Sadeghzadeh RA. Novel microstrip patch antenna to use in 2×2 sub arrays for DBS reception. *Indian Journal of Science and Technology*. 2012 Jul; 5(7).
- [7] Elt ouh H, Touhami NA, Aghoutane M. Miniaturized microstrip patch antenna with defected ground structure. *Progress in Electromagnetic Research C*. 2014; 55:25–33.
- [8] Noelia Ortiz, Francisco Falcone, Mario Sorolla, Gain improvement of dual band antenna based on complementary rectangular split-ring resonator, *ISRN Communications and Networking* 3 (2012).
- [9] Jagannath Malik, Machavaram Venkata Kartikeyan, Metamaterial inspired patch antenna with L-shape slot loaded ground plane for dual band (WiMAX/WLAN) applications, *Prog. Electromagn. Res.* 31 (2012) 35–43.
- [10] C. Yeh, G.D. Jo, Y. Ko, H.K. Chung, Perspectives on 6G Wireless Communications, *ICT Express*, 2022 in press.
- [11] S.C. Basaran, Ulgur Olgun, Sertel Kubilay, Multiband monopole antenna with complementary split-ring resonators for WLAN and WiMAX applications, *Electron. Lett.* 49 (10) (2013) 636–638.
- [12] A. Dejen, M. Ridwan, J. Anguera, J. Jayasinghe, Millimeter wave cellular communication performances and challenges: a survey, *EAI Endorsed Trans. Mob. Commun. Appl.* 7 (2022) e5.
- [13] A. Sahaya Anselin Nisha, M. Saravanan, K. Sakthisudhan, D. Vijendra Babu, Epoxy based textile 3x3 grid microstrip slots & breast tumor coverage detection by composites, *Mater. Today: Proc.* 45 (7) (2021) 6623–6627.
- [14] B. Jackson, T. Jayanthi, Moisture content determination using microstrip fractal resonator sensor, *Res. J. Appl. Sci. Eng. Technol.* 7 (14) (2014) 2994–2997. No: 0034- 6748(P) 1089-7623(O).
- [15] A.A. Roseline, K. Malathi, A.K. Shrivastav, Enhanced Performance of a Patch Antenna Using Spiral-Shaped Electromagnetic Bandgap Structures for High-Speed Wireless Networks" - *IET Microwaves, antennas & propagation*, 2011.